Single-beam squeezed-state generation in semiconductor waveguides with $\chi^{(3)}$ nonlinearity at below half-band gap

Seng-Tiong Ho, Xiaolong Zhang, and Maria K. Udo

*Department of Electrical Engineering and Computer Science,
Northwestern University, Evanston, Illinois 60208*

We analyze a new scheme for generating squeezed states in a short semiconductor $Al_x Ga_{1-x}As$ waveguide with $\chi^{(3)}$ nonlinearity at below half the band-gap energy. We find that for a Gaussian pulse the amount of squeezing achievable is limited by the squeezed-state detection phase mismatch caused by the pump self-phase modulation and is also degraded slightly by the pump–probe phase mismatch that is due to the different nonlinear refractive indices experienced by the pump and the probe beams. We show theoretically that the amount of squeezing observed can be increased by use of either a short pulse or a pulse with matched phase variation as the local oscillator. In a centimeter-long $Al_x Ga_{1-x}As$ waveguide more than 85% (8.2 dB) of squeezing potentially can be obtained, limited mainly by two-photon absorption.

1. INTRODUCTION

We analyze in detail the generation of squeezed-state light in semiconductor waveguides with $\chi^{(3)}$ nonlinearity at below half the band-gap energy. Because of the low two-photon absorption below half the band-gap energy, we find that a substantial amount of squeezing can be achieved. However, the use of Gaussian pump pulses can seriously limit the amount of observed squeezing if the input laser beam is used as the local oscillator (LO). Various methods to improve the amount of observed squeezing with different types of LO beams are analyzed and discussed.

2. BACKGROUND AND MOTIVATION

It has been shown that squeezed-state light can be used to circumvent the shot-noise limit and consequently to enhance the ultimate sensitivity of an interferometer,[1] reduce the bit error rate, and increase the channel capacity of quantum communication systems.[2,3] Squeezed-state light has been generated in both $\chi^{(2)}$ and $\chi^{(3)}$ media.[4–11] Compared with $\chi^{(3)}$ media, $\chi^{(2)}$ media usually have several advantages, such as their high nonlinearity and generally fast response time and low losses, which enable one to generate large amounts of squeezing. However, in $\chi^{(2)}$ media the squeezed-state sidebands generated are centered at a frequency ν_s that is half the frequency of the pump light ν_e. Because the LO beam that one needs to detect the squeezed-state sidebands through homodyne detection must have a frequency equal to ν_s, frequency doubling is needed for generation of the pump beam so that part of the original beam at half of the pump frequency can be used as the LO. Moreover, because the pump beam does not have the same frequency as the LO beam, it cannot be reused as the LO and is therefore wasted after the generation of squeezing. On the other hand, squeezed-state light generated in $\chi^{(3)}$ media has the same frequency as the pump, thus eliminating the need for additional frequency conversion. In addition, the pump can be reused as the LO in subsequent homodyne detection. Hence one may expect that if squeezed-state light were successfully generated in $\chi^{(3)}$ media, simpler squeezed-states generation schemes could be constructed.

In spite of the above-mentioned promise of simplicity, attempts to generate squeezed-state light in $\chi^{(3)}$ media have encountered various difficulties. In the following we review some of the problems discussed in the literature relative to the use of $\chi^{(3)}$ media to generate squeezing. We also discuss the various solutions attempted, which will be related to our interest in investigating the feasibility of squeezed-state generation in $\chi^{(3)}$ semiconductor waveguides. For example, in the early attempts to generate squeezed states in $\chi^{(3)}$ media it was found that systems such as atomic vapor, which use interaction geometries involving beam propagation in free space, are limited by the differential nonlinear focusing effect between the pump and the probe beams (the probe beams are the squeezed vacuum beams).[10] This nonlinear focusing effect is due to the lenslike refractive index in the medium induced by the Gaussian pump beam intensity through the nonlinear (intensity-dependent) refractive index inherent in $\chi^{(3)}$ media. The differential nonlinear focusing effect is due to the fact that the strong pump and weak probe beams see a factor-of-2 difference in the nonlinear refractive indices and hence experience different focusing in spite of the fact that they have the same frequency and polarization.[12] A more familiar context having the same origin as the nonlinear focusing effect is the factor-of-2 difference between (the pump's) self-phase modulation and (pump-induced) cross-phase modulation on the probe.[12–14] This difference in nonlinear focusing is detrimental to squeezing because when the pump intensity is high enough to create a large amount of squeezing it is also high enough to create a strong differential focusing between the pump and probe beams, which seriously reduces the spatial overlap between them, thereby

leading to weak interaction and hence to weak squeezing. One way to overcome the differential nonlinear focusing is to confine the pump and the probe beams in an optical waveguide. The use of a waveguide helps because the nonlinear change in the spatial profiles of the waveguide refractive indices (as seen by the pump and the probe beams) induced by the pump is in general weak compared with the waveguide core-to-cladding step index difference and hence will not substantially affect waveguiding. This means that in a single-mode waveguide the pump and the probe beams will remain spatially well overlapped (highly mutlimode waveguides will degenerate to free-space propagation). We should mention that, although the differential nonlinear focusing problem is eliminated with the use of a single-mode waveguide, there is an associated effect that still remains. It is the factor-of-2 difference between self-phase modulation and cross-phase modulation mentioned above that causes the pump and the probe beams to experience different nonlinear phase shifts. This difference in nonlinear phase shift can give rise to the (nonlinear) pump–probe phase mismatch in four-wave mixing interaction that is responsible for the parametric gain needed to produce squeezing.[12,13] As a result, the presence of nonlinear pump–probe phase mismatch will lead to a reduction in the effective interaction strength for a given medium length, resulting in reduced squeezing. It turns out that the problem of nonlinear pump–probe phase mismatch is not a fundamental one, as one can compensate for it by increasing the medium length (i.e., it does not impose a maximum limit on the amount of squeezing achievable).[12] However, as we discuss below, in a lossy medium this increase in medium length can give rise to increased losses, which will reduce the amount of squeezing.

The early attempts to generate squeezed-state light with waveguides made use of optical fibers as the nonlinear waveguiding media.[5] However, it was later found that there was a problem associated with the use of fibers because of the presence of additional noise from guided acoustic-wave Brillouin scattering (GAWBS),[15,16] which is inherent in all solid waveguiding media. This noise results from the random phase modulation of the incident light by the thermally excited vibrational eigenmodes that modulate the refractive index of the waveguide. The optical noise power generated by GAWBS is proportional to the length of the waveguide.[15] Because a long fiber length is needed to generate substantial amounts of squeezing, the effect of GAWBS noise can be serious enough to mask the observation of quantum noise reduction or squeezing. In fact, the early squeezed-state generation experiments in fiber were seriously limited by GAWBS noise.[5] It turns out that GAWBS noise can be reduced by various methods such as cooling down the fiber. Recently it was shown that GAWBS noise could also be reduced by the use of short pulses instead of a continuous-wave (cw) beam to generate the squeezed state.[17] Short pulses help to reduce GAWBS noise because the excess phase noise resulting from the slow thermal refractive-index fluctuations scales linearly with the average power of the pulse train, whereas nonlinear effects such as squeezing scale with the peak power of the pulse.[17–19] Thus less GAWBS noise will be generated by use of a pulse train with low average power. Moreover,

the use of high-intensity pulses allows one to use a shorter length of waveguide, resulting in reduced GAWBS noise power. Recently it was also pointed out that the use of pump pulses with a gigahertz repetition rate can decrease GAWBS noise by reducing the folding over of the high-frequency GAWBS noise that occurs when a megahertz pulse train is used (the GAWBS noise spectrum generally extends to the gigahertz frequency range).[20] It was also found recently that some fibers actually generate much less GAWBS noise at certain frequencies[21,22] and that GAWBS noise can be partially canceled out at the homodyne detection by use of a dual-pulse-excitation scheme in a fiber.[23,24] The dual-pulse-excitation scheme reduces the GAWBS noise detected by generation of pairs of squeezed vacuum pulses and LO pulses that possess the same phase modulation induced by the GAWBS noise.

Although the use of high-intensity pulses can assist in the reduction of GAWBS noise and also compensate for the generally low nonlinearity of $\chi^{(3)}$ media, it is not without penalty. It turns out that using nonsquare pump pulses such as the Gaussian pulses can seriously affect the amount of squeezing observable. This is basically because the phase quadrature angle at which the maximum squeezing is generated is a function of the pump intensity. The phase quadrature angle is usually specified relative to the pump phase before the medium (because the input pump phase is the only phase reference in the system). For a cw pump beam with intensity I_p, let us call the phase quadrature angle at which maximum squeezing is generated (at the medium's output) $\Phi_M(I_p)$, where $\Phi_M(I_p)$ takes values between 0 and π (the squeezed quadrature angle is unique only up to a phase of π) and $\Phi_M = 0$ corresponds to the case when the phase quadrature is in phase with the input pump. To detect the maximum amount of squeezing for the cw pump one has to tune the phase of the LO, which is also a cw beam, to $\Phi_M(I_p)$. If the pump beam does not experience self-phase modulation, then the value of $\Phi_M(I_p)$ is dependent only on the nature of the intensity-dependent four-wave mixing interaction. In the case when the pump experiences an additional nonlinear phase shift that is due to self-phase modulation, there will be a corresponding additional phase shift to $\Phi_M(I_p)$ (simply because the squeezed quadrature is relative to the pump phase), which will be referred to as $\Phi_M^{SPM}(I_p)$. So in general we can write $\Phi_M(I_p)$ as a sum of two parts: $\Phi_M(I_p) = \Phi_M^{SPM}(I_p) + \Phi_M^{FWM}(I_p)$, in which $\Phi_M^{FWM}(I_p)$ is the part that is due solely to four-wave mixing interaction.[25] For $\chi^{(2)}$ media $\Phi_M^{SPM}(I_p)$ is generally absent. For $\chi^{(3)}$ media the presence of Φ_M^{SPM} makes $\Phi_M(I_p)$ more intensity dependent, which can seriously affect the detection of pulsed squeezing.

The problem of $\Phi_M(I_p)$ on pulsed squeezing is as follows: Because $\Phi_M(I_p)$ is intensity dependent, the value of $\Phi_M(I_p)$ will vary across the pump pulse according to the pump pulse intensity variation when a nonsquare pump pulse is used. Correspondingly, for the maximum squeezing for the whole squeezed pulse to be detectable the LO pulse is required to have a phase variation matching the values of $\Phi_M(I_p)$ across the squeezed pulse. An ordinary unchirped, transform-limited LO pulse with a uniform phase under its pulse profile cannot meet this phase-matching requirement, and consequently phase mismatch is introduced. We refer to this as the

squeezed-state detection (SSD) phase mismatch. Owing to SSD phase mismatch, less squeezing or even noise will be detected when a transform-limited LO pulse is used, and the observed squeezing for the whole pulse is thus reduced. In the case of fiber squeezing with a Gaussian pulse it was found that the amount of squeezing observed[23] was increased when the output pump pulse was used as the LO. When the output pump pulse is used as the LO the LO pulse will have a nonlinear phase chirp under its pulse envelope as a result of the pump's self-phase modulation, which exactly cancels the part of SSD phase mismatch that is due to the $\Phi_M^{\mathrm{SPM}}(I_p)$ part of $\Phi_M(I_p)$. The SSD phase mismatch that is due to the $\Phi_M^{\mathrm{FWM}}(I_p)$ part of $\Phi_M(I_p)$, however, is not canceled and will still impose some limit on the observed squeezing. The problem of SSD phase mismatch caused by Φ_M^{FWM} and its solution are discussed below. Before we leave this section, it should be pointed out that the use of lowest-order optical solitons as the pump pulses can also avoid the SSD phase-mismatch component that is due to Φ_M^{SPM} because the lowest-order optical solitons do not suffer from the pulse chirping problem.[26]

To obtain large amounts of squeezing by using a $\chi^{(3)}$ nonlinearity it is necessary to address the problems discussed above judiciously. The proper choice of the $\chi^{(3)}$ material and structure and the careful design of the experimental scheme, including a proper choice of LO pulses, need to be considered carefully.

The maximum amount of squeezing achieved in atomic vapor, which was the first medium used to generate squeezing,[4] is approximately 25%, or 1.2 dB,[10] and this value is limited by the nonlinear differential focusing. Rosenbluh and Shelby pioneered squeezing in optical fibers by the use of optical solitons.[26] However, the maximum amount of squeezing in their experiments has been limited to 32% (1.7 dB) because of serious GAWBS noise and SSD phase mismatch owing to $\Phi_M^{\mathrm{FWM}}(I_p)$. Recently a great improvement in the amount of squeezing observed in optical fibers was achieved by Bergman *et al.*[20–23] By injecting pulses into a nonlinear Mach–Zehnder fiber interferometer, they achieved squeezing as high as 5.1 dB. To circumvent GAWBS noise they used a special fiber yielding very low GAWBS noise,[21,22] or pump pulses with a gigahertz repetition rate that is out of the bandwidth of the GAWBS,[20] or a dual-pulse-excited fiber ring to cancel out GAWBS noise.[23] The SSD phase-mismatch component that is due to Φ_M^{SPM} is canceled out in their experiments because the output pump pulse from the fiber interferometer is reused as the LO pulse in homodyne detection. However, the SSD phase mismatch that is due to $\Phi_M^{\mathrm{FWM}}(I_p)$ still remains. Our numerical results in this paper show that this residual SSD phase mismatch can reduce squeezing by more than 10%.

In this paper we propose a new scheme of generating squeezed-state light by using an $\mathrm{Al}_x\mathrm{Ga}_{1-x}\mathrm{As}$ waveguide with $\chi^{(3)}$ nonlinearity[27] and present the results of our theoretical study on the amount of squeezing achievable in such a waveguide. The unique feature of the $\mathrm{Al}_x\mathrm{Ga}_{1-x}\mathrm{As}$ semiconductor waveguide, compared with a fiber, is that a substantial amount of squeezing can be achieved in centimeter-long $\mathrm{Al}_x\mathrm{Ga}_{1-x}\mathrm{As}$ semiconductor waveguides with negligible GAWBS noise. This makes it possible to build a compact and simple scheme with

an $\mathrm{Al}_x\mathrm{Ga}_{1-x}\mathrm{As}$ semiconductor waveguide to generate squeezing. It turns out that with the same pump power the waveguide length needed to generate large amounts of squeezing in an $\mathrm{Al}_x\mathrm{Ga}_{1-x}\mathrm{As}$ semiconductor waveguide is approximately 10^4 times less than that in a silica fiber. The reason is twofold. First, the nonlinear four-wave mixing gain coefficient of $\mathrm{Al}_x\mathrm{Ga}_{1-x}\mathrm{As}$ is 100 times that of typical optical fibers. Second, the mode cross-sectional area of a single-mode $\mathrm{Al}_x\mathrm{Ga}_{1-x}\mathrm{As}$ rib waveguide is approximately 100 times smaller than that of a single-mode fiber. The much smaller cross-sectional area is a result of the higher material refractive index and stronger optical confinement found in $\mathrm{Al}_x\mathrm{Ga}_{1-x}\mathrm{As}$ semiconductor waveguides than in optical fibers. Because of the short length of the semiconductor waveguide, GAWBS noise will be negligible.[15,28] This eliminates the additional apparatus and techniques needed to combat GAWBS noise and further simplifies the experimental setup for generating squeezing in semiconductor waveguides.

To combat the SSD phase mismatch, besides the reused pump scheme we analyze two other schemes in this paper. We show that, besides the LO pulse from the reused pump pulse, there are two kinds of LO pulse that can be used to minimize further the SSD phase mismatch. One is a short LO pulse whose width is narrower than that of the pump pulse or the squeezed vacuum pulse; the other is a nearly matched LO pulse whose nonlinear phase variation is optimized in another similar semiconductor waveguide to cancel out SSD phase mismatch. We show that both of the schemes can yield a higher degree of squeezing than the reused pump scheme (the narrow LO scheme requires the LO pulse width to be approximately one eighth (or less than one eighth) that of the pump pulse to yield a substantial advantage).

Losses are also considered in this paper, which are potentially problems for the generation of large amounts of squeezing in semiconductor waveguides. Typically, the linear loss for a high-quality $\mathrm{Al}_x\mathrm{Ga}_{1-x}\mathrm{As}$ semiconductor rib waveguide is a few decibels per centimeter. This is much larger than the typical linear loss of an optical fiber, which can be as low as 0.2 dB/km. However, the length of the semiconductor waveguide required for generation of a large amount of squeezing is usually no more than a few centimeters. As a result, the linear loss of the whole waveguide is still small and is not a serious problem. Besides linear loss, another important loss comes from nonlinear absorption, including two-photon absorption and three-photon absorption. Two-photon absorption is proportional to the pump intensity, and three-photon absorption is proportional to the square of the pump intensity. As a result, the absorption can be large enough to destroy squeezing when the pump intensity is too high. For a $\chi^{(3)}$ medium to be useful for squeezed-state generation, its nonlinear loss must be small at the pump intensity that is needed to generate a substantial amount of squeezing. Because of the relation between the four-wave mixing gain coefficient and the nonlinear refractive index[29] it turns out that when the pump intensity is high enough to generate a substantial amount of squeezing it is also high enough to cause the pump to experience a nonlinear phase shift of the order of π. The nonlinear phase shift is given by $\delta\Phi_{\mathrm{NL}} = 2\pi n^{(2)} I_p l/\lambda$, where $n^{(2)}$ is the non-

linear refractive index, I_p is the pump intensity, and l is the medium length. The medium absorption is given by $\alpha(I_p)l$, where $\alpha(I_p)l$ is the intensity-dependent loss. For a given pump intensity I_p the medium length needed to yield π phase shift is given by $l = \lambda/[2n^{(2)}I_p]$, at which the loss will be $\alpha(I_p)l = \alpha(I_p)\lambda/[2n^{(2)}I_p]$. For the medium to be useful for squeezing, we want this loss to be smaller than unity. Let us define a figure of merit $F \equiv 1/G$, where $G \equiv \lambda\alpha(I_p)/[2n^{(2)}I_p]$ (G will be called the inverse figure of merit). For the loss to be smaller than unity we must have $G < 1$, which is the condition needed for the medium to be useful for squeezing. $\alpha(I_p)$ can be expanded as $\alpha(I_p) = \alpha^{(1)} + \alpha^{(2)}I_p + \alpha^{(3)}I_p^2 + \ldots$, where $\alpha^{(1)}$, $\alpha^{(2)}$, and $\alpha^{(3)}$ are the linear, two-photon, and three-photon absorption coefficients, respectively. We can write $G = G_1 + G_2 + G_3 + \ldots$, where $G_n \equiv \lambda\alpha^{(n)}I_p^{(n-1)}/[2n^{(2)}I_p]$ is the nth-photon inverse figure of merit, which is the inverse figure of merit when nth photon absorption is dominating. Whereas all the G_n with $n \neq 2$ are dependent on the pump intensity I_p, G_2 is independent of I_p and is dependent solely on the material property given by the ratio between the two-photon absorption coefficient $\alpha^{(2)}$ and the nonlinear refractive index $n^{(2)}$. Clearly the value of F is fundamentally lower bounded by $1/G_2$ and hence by the material two-photon absorption. Three-photon absorption alone is not a fundamental limitation to F, as one can reduce the value of F_3 by reducing the pump intensity I_p {which means an increase in the required medium length l, as l is related to I_p by $l = \lambda/[2n^{(2)}I_p]$}. However, when the linear absorption is high, $G_1 + G_3$ is a fundamental limitation to F, as G_1 is inversely proportional to I_p and G_3 is proportional to I_p, and hence there is a lower bounded value for $G_1 + G_3$. Semiconductors are known to have large $\chi^{(3)}$ at just below the band-gap energy. However, in that region the two-photon absorption coefficient is high, giving a low figure of merit F. Recently it was shown that, if one operates at the frequency region below half the band-gap energy, two-photon absorption will be drastically reduced while $\chi^{(3)}$ is only slightly reduced, giving a large figure of merit. For example, a $Al_xGa_{1-x}As$ semiconductor waveguide operating at just below half the band-gap energy (with pump wavelength at 1.55 μm) has $n^{(2)} = (3.6 \pm 0.5) \times 10^{-14}$ cm^2/W, $\alpha^{(2)} = 0.26 \times 10^{-4}$ cm/MW, and $\alpha^{(3)} = 0.004$ cm^3/GW^2.[27] With a 1-cm-long waveguide it turns out that $\alpha^{(2)}$ is the main contribution to F, giving $F \simeq 5$. Because of this high figure of merit our numerical results in this paper show that for the case of an $Al_xGa_{1-x}As$ waveguide operating below half the band-gap energy a large amount of squeezing can be achieved. The maximum amount of squeezing achievable is 10% lower than for the ideal lossless case and is limited mainly by the two-photon absorption. For three-photon absorption it can be large for the case of short waveguides, for which one may need high pump intensity to achieve a π phase shift. However, in the case of an $Al_xGa_{1-x}As$ waveguide we found that the three-photon absorption coefficient is low enough that its effect is negligible for the intensity required for a nonlinear π phase shift in a centimeter-long waveguide.

The contents of this paper are as follows. In Section 3 we review the theory of generating a squeezed state in a guided $\chi^{(3)}$ medium through nearly degenerate four-wave mixing (NDFWM) processes. We show the origin

and the effects of pump–probe phase mismatch and SSD phase mismatch. In Section 4, through numerical calculations, we further analyze the effects of these two kinds of phase mismatch and nonlinear absorption. We show that the effect of pump–probe phase mismatch is very small, whereas SSD phase mismatch is the most important effect. We discuss various schemes to combat SSD phase mismatch in detail. In Section 5 we present our conclusions.

3. THEORETICAL BACKGROUND: SQUEEZED-STATE GENERATION IN A GUIDED $\chi^{(3)}$ MEDIUM THROUGH NEARLY DEGENERATE FOUR-WAVE MIXING

The scheme for the generation of squeezed light in a waveguide is shown in Fig. 1. A single strong pump beam E_p with two vacuum sidebands, to which we refer as probe signal beam $\hat{a}_s$ and probe conjugate beam $\hat{a}_{s'}$, respectively, is sent into the waveguide. The frequencies of $\hat{a}_s$ and $\hat{a}_{s'}$, given by ω_s and $\omega_{s'}$, satisfy $2\omega_p = \omega_s + \omega_{s'}$ and are nearly degenerate with ω_p. Here we consider the four-wave mixing process in the nearly degenerate region where the frequency detuning of ω_s from ω_p (or of $\omega_{s'}$ from ω_p) is smaller than the inverse of the medium's nonlinear response time τ_M (i.e., $|\omega_p - \omega_s| \ll 1/\tau_M$).[30] For an $Al_xGa_{1-x}As$ waveguide τ_M can be considered instantaneous, as it is of the order of 200 fs or faster. Through the NDFWM process the two probe beams are transformed into squeezed vacuum at the output end of the waveguide, similar to the case of single-beam squeezed-state generation in atomic vapor.[4,10,12] For plane waves the NDFWM process can be described by the following equations[12,13]:

$$\frac{\partial E_p}{\partial z} = i\kappa_p I_p E_p, \tag{1}$$

$$\frac{\partial \hat{a}_s}{\partial z} = -\gamma\hat{a}_s + i\kappa_s I_p \hat{a}_s + iX_s I_p \exp(i2\kappa_p I_p z)\hat{a}_{s'}^\dagger + \hat{G}_s(z), \tag{2}$$

$$\frac{\partial \hat{a}_{s'}^\dagger}{\partial z} = -\gamma\hat{a}_{s'}^\dagger - i\kappa_s I_p \hat{a}_{s'}^\dagger - iX_s^* I_p \exp(-i2\kappa_p I_p z)\hat{a}_s + \hat{G}_{s'}^\dagger(z). \tag{3}$$

We should note here that the dispersion terms were neglected in the above equations. The reason for this neglect is that dispersion effects are negligible for the material used in our specific investigation. We have found experimentally that dispersion effects are negligible for pulses propagating in a 1-cm-long AlGaAs waveguide at half the band-gap energy, provided that the pulse length is longer than 100 fs. In the calculations presented in this paper the pulses are 500 fs wide, which is in the region where dispersion effects are negligible. Therefore in this paper we neglect the dispersion effects.

Here we treat the pump as a classical field, neglecting its loss. The probe beams $\hat{a}_s$ and $\hat{a}_{s'}$ are quantized. In the above equations $I_p = E_p^* E_p$ is the pump intensity, $\gamma = 2[\alpha^{(2)} + \alpha^{(3)}I_p]I_p$ is the nonlinear absorption coefficient including both two- and three-photon absorption, and X_s is the nonlinear coupling coefficient. In the nearly degenerate frequency limit X_s has a simple relation to κ_s
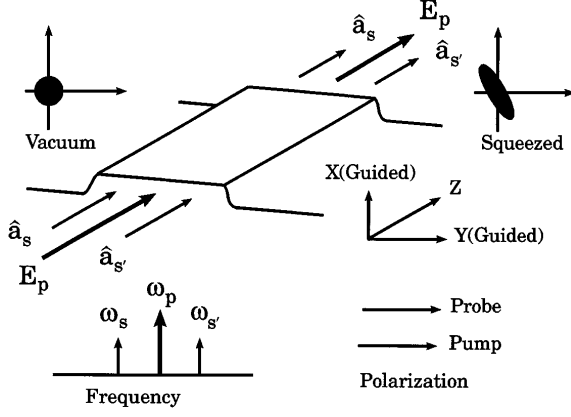
Fig. 1. Scheme to generate squeezing in an $Al_xGa_{1-x}As$ waveguide. E_p is a strong classical pump, and $\hat{a}_s$ and $\hat{a}_{s'}$ are its vacuum sidebands (quantized probes).

and γ and is given by $X_s = (1/2)[\kappa_s + i(\gamma/I_p)]$.[12] The nonlinear coefficients for the pump and the two probe beams are κ_p and κ_s, respectively, and are proportional to the nonlinear refractive index $n^{(2)}$ experienced by the pump. For the case in which the polarizations of the pump and the probe fields are the same, they are related by $\kappa_s = 2\kappa_p = (4\pi/\lambda)n^{(2)}$. As discussed above, the factor of 2 between κ_s and κ_p will give nonlinear pump–probe phase mismatch, which reduces the parametric gain of the probe beams. Because we are in the NDFWM region we can assume that the two probe beams have the same γ, κ_s, and X_s. The Langevin noise terms that are due to losses are denoted $\hat{G}_s(z)$ and $\hat{G}_{s'}^\dagger(z)$, with $[\hat{G}_\alpha(z), \hat{G}_\beta^\dagger(z')] = 2\gamma\delta_{\alpha\beta}\delta(z - z')$ and $\alpha, \beta = s, s'$.

In our calculations we take the effect of the waveguide into account by introducing mode overlapping integrals into the nonlinear terms of the above equations. Let $u_p(x, y)$, $u_s(x, y)$, and $u_{s'}(x, y)$ be the transverse spatial mode profiles of the pump and the two probe beams, respectively. The equation for $\hat{a}_s(z)$ in the waveguide can be written as follows:

$$\frac{\partial \hat{a}_s}{\partial z} = -2[\alpha^{(2)}I_p F_s^{(2)} + \alpha^{(3)}I_p^2 F_s^{(3)}]$$
$$\times \hat{a}_s + i\kappa_s I_p F_s^{(2)}\hat{a}_s + iX_s I_p F_s^{(2)}$$
$$\times \exp(i2\kappa_p F_p^{(2)} I_p z)\hat{a}_{s'}^+ + \hat{G}_s(z), \qquad (4)$$

where

$$F_s^{(2)} = \frac{\iint u_s(x, y)u_p^2(x, y)u_{s'}(x, y)\,dxdy}{\iint u_s^2(x, y)\,dxdy}. \qquad (5)$$

In a similar way, modified equations for E_p and $\hat{a}_{s'}$ can be obtained by the use of similar mode overlapping integrals $F_p^{(2)}$ and $F_{s'}^{(2)}$, respectively. In our case we assume only the lowest-order guided modes, and we can make the following approximations: $u_p(x, y) = u_s(x, y) = u_{s'}(x, y) = \cos(k_x x)\cos(k_y y)$ and $F_p^{(2)} = F_s^{(2)} = F_{s'}^{(2)} = 0.5625$, where $k_x = \pi/d_x$, $k_y = \pi/d_y$, and d_x and d_y are the transverse dimensions of the waveguide. In Eq. (4) we have included both the two-photon absorption term $\alpha^{(2)}$ and the three-photon absorption term $\alpha^{(3)}$. We can obtain the corresponding overlapping integral $F_s^{(3)}$ for the $\alpha^{(3)}$ term by replacing the integrand $u_p^2(x, y)$ in Eq. (5) with $u_p^4(x, y)$.

To see the origin of the nonlinear pump–probe phase mismatch clearly, we perform a slowly varying amplitude approximation $\hat{a}_s = \tilde{a}_s \exp[i\kappa_s F_s^{(2)}I_p z]$, $\hat{a}_{s'}^\dagger = \tilde{a}_{s'}^\dagger \exp[-i\kappa_s F_s^{(2)}I_p z]$ to transform away the fast varying imaginary part [term $i\kappa_s F_s^{(2)}I_p$ in Eq. (4)]:

$$\frac{\partial \tilde{a}_s}{\partial z} = -\gamma\tilde{a}_s + iX_s I_p \exp[i2(\kappa_p - \kappa_s)I_p z]$$
$$\times \tilde{a}_{s'}^\dagger + \hat{G}_s(z)\exp(-i\kappa_s I_p z), \qquad (6)$$

$$\frac{\partial \tilde{a}_{s'}^\dagger}{\partial z} = -\gamma\tilde{a}_{s'}^\dagger - iX_s^* I_p \exp[-i2(\kappa_p - \kappa_s)I_p z]$$
$$\times \tilde{a}_s + \hat{G}_{s'}^\dagger(z)\exp(i\kappa_s I_p z), \qquad (7)$$

where γ, X_s, κ_p, and κ_s are taken to be their new values with the overlapping integrals included. The phase mismatch between the pump and the probe beams is denoted $\Delta\kappa = 2(\kappa_x - \kappa_p)I_p$. It originates from the different nonlinearities experienced by the pump and the probe beams.

To solve the coupled-mode equations (6) and (7) we define $\hat{b}_s$ and $\hat{b}_{s'}$ through $\tilde{a}_s = \hat{b}_s \exp(-i\Delta\kappa z/2)$, $\tilde{a}_{s'}^\dagger = \hat{b}_{s'}^\dagger \exp(i\Delta\kappa z/2)$, in terms of which we obtain the following equations with constant coefficients:

$$\frac{\partial \hat{b}_s}{\partial z} = (-\gamma + i\Delta\kappa/2)\hat{b}_s + iX_s I_p \hat{b}_{s'}^\dagger + \hat{G}_s \exp(-i\kappa_p I_p z), \qquad (8)$$

$$\frac{\partial \hat{b}_{s'}^\dagger}{\partial z} = (-\gamma - i\Delta\kappa/2)\hat{b}_{s'}^\dagger - iX_s^* I_p \hat{b}_s + \hat{G}_{s'}^\dagger \exp(i\kappa_p I_p z). \qquad (9)$$

Equations (8) and (9) can be readily solved by standard linear algebra, giving us the solutions for $\hat{b}_s(z)$ and $\hat{b}_{s'}^\dagger(z)$.[12,13] After that, we transform $\hat{b}_s$ and $\hat{b}_{s'}^\dagger$ back to $\hat{a}_s$ and $\hat{a}_{s'}^\dagger$, resulting in

$$\hat{a}_s(l) = \exp(-\gamma l)\exp(i\kappa_p I_p l)[\mu(l)\hat{a}_s(0) + \nu(l)\hat{a}_{s'}^\dagger(0)]$$
$$+ \hat{\Gamma}_1(l)\exp(i\kappa_p I_p l), \qquad (10)$$

$$\hat{a}_{s'}^\dagger(l) = \exp(-\gamma l)\exp(-i\kappa_p I_p l)[\mu^*(l)\hat{a}_{s'}^\dagger(0) + \nu^*(l)\hat{a}_s(0)]$$
$$+ \hat{\Gamma}_2^\dagger(l)\exp(i\kappa_p I_p l), \qquad (11)$$

where we have set $z = l$ as the waveguide length and

$$\mu(l) = \cosh(\Omega l) + (i\Delta\kappa/2\Omega)\sinh(\Omega l), \qquad (12)$$

$$\nu(l) = (iX_s I_p/\Omega)\sinh(\Omega l), \qquad (13)$$

$$\Omega = (|X_s I_p|^2 - \Delta\kappa^2/4)^{1/2}, \qquad (14)$$

$$\hat{\Gamma}_1(l) = \int_0^l dz' \exp[-\gamma(l - z')][\exp(-i\kappa_p I_p z')$$
$$\times \mu(l - z')\hat{G}_s(z') + \exp(i\kappa_p I_p z')$$
$$\times \nu(l - z')\hat{G}_{s'}^\dagger(z')], \qquad (15)$$

$$\hat{\Gamma}_2^\dagger(l) = \int_0^l dz' \exp[-\gamma(l - z')][\exp(i\kappa_p I_p z')$$
$$\times \mu^*(l - z')\hat{G}_{s'}^\dagger(z') + \exp(-i\kappa_p I_p z')$$
$$\times \nu^*(l - z')\hat{G}(z')]. \qquad (16)$$

In Eqs. (10) and (11) the canonical transformation described by the square-bracketed terms is called a

Bogoliubov transformation. Note here that, with non-linear absorption and nonlinear pump–probe phase mismatch, both of the coefficients of the Bogoliubov transformation, $\mu(l)$ and $\nu(l)$, are complex. Equation (14) shows that the parametric gain Ω is reduced by the nonlinear pump–probe phase mismatch $\Delta\kappa$.

To calculate the amount of squeezing at a particular phase quadrature of the probes, we define the phase quadrature operator for the probes as follows:

$$\hat{X}(\varphi) = [(\hat{a}_s + \hat{a}_{s'})\exp(-i\varphi) + (\hat{a}_s^\dagger + \hat{a}_{s'}^\dagger)\exp(i\varphi)]/(2\sqrt{2}),$$
(17)

where φ is the relative phase between the LO beam and the input pump beam, which will be simply referred to as the LO phase. The detector photocurrent output of a homodyne detection system gives the fluctuation of the probe quadrature that can be calculated by using Eqs. (10) and (11):

$$\langle[\Delta\hat{X}(\varphi)]^2\rangle = 1/4 + 1/2[c + \sqrt{a^2 + b^2}$$
$$\times \sin(2\varphi - 2\kappa_p I_p l + \Phi_{ab})], \quad (18)$$

where

$$a = \exp(-2\gamma l)\mathrm{Re}(\mu\nu) + \mathrm{Re}(\langle\hat{\Gamma}_1\hat{\Gamma}_2\rangle), \quad (19)$$

$$b = \exp(-2\gamma l)\mathrm{Im}(\mu\nu) + \mathrm{Im}(\langle\hat{\Gamma}_1\hat{\Gamma}_2\rangle), \quad (20)$$

$$c = \exp(-2\gamma l)|\nu|^2 + \langle\hat{\Gamma}_1^+\hat{\Gamma}_1\rangle, \quad (21)$$

$$\Phi_{ab} = \arctan(a/b). \quad (22)$$

The expressions for $\mathrm{Re}(\mu\nu)$, $\mathrm{Im}(\mu\nu)$, $\mathrm{Re}(\Gamma_1\Gamma_2)$, $\mathrm{Im}(\Gamma_1\Gamma_2)$, $|\nu|^2$, and $\langle\Gamma_1^\dagger\Gamma_1\rangle$ are given in Appendix A.

The amount of squeezing as a percent is defined as

$$S = [1 - 4\langle(\Delta X(\varphi)]^2\rangle] \times 100\%. \quad (23)$$

Squeezing is achieved whenever $\langle[\Delta\hat{X}(\varphi)]^2\rangle < 1/4$ or $S > 0$. From Eq. (18) we see that the amount of squeezing achievable is affected by two factors: (1) the phase of the $\sin[2\varphi - 2\kappa_p I_p l + \Phi_{ab}(I_p)]$ term and (2) the amplitude, given by $\sqrt{a^2 + b^2}$. Note that the $-2\kappa_p I_p l$ phase term comes from the nonlinear phase shift of the pump $\kappa_p I_p l$ after waveguide length l, whereas the $\Phi_{ab}(I_p)$ term originates from the four-wave mixing process. They are the Φ_M^{SPM} and Φ_M^{FWM} terms mentioned in Section 1 [i.e., $\Phi_M^{\mathrm{SPM}}(I_p) = \kappa_p I_p l$ and $\Phi_M^{\mathrm{FWM}}(I_p) = \Phi_{ab}(I_p)$]. The probe nonlinear phase affects only the pump–probe phase mismatch $\Delta\kappa$, which is embedded in variables a, b, c, and Φ_{ab}. For a given amplitude, maximum squeezing occurs when $\sin(2\varphi - 2\kappa_p I_p I + \Phi_{ab}) = -1$, leading to the phase-matching condition

$$2\varphi - 2\kappa_p I_p l + \Phi_{ab} = 2n\pi - \pi/2. \quad (24)$$

Equation (24) describes the SSD phase-matching condition. We see that detecting maximum squeezing requires an appropriate LO phase φ. The simplest case is described by a square pump pulse, where both $-2\kappa_p I_p l$ and $\Phi_{ab}(I_p)$ are constant for the entire pulse so that a single phase value φ can meet the SSD phase-matching condition across the whole pulse. Physically, this means that the LO pulse that satisfies the SSD phase-matching

condition across the entire pulse will be one that has an unchirped uniform sine wave under the LO pulse envelope. Such a LO pulse will be referred to as a uniform-phase LO. Hence, for a square pump pulse or a cw pump, the SSD phase-matching condition can be easily satisfied experimentally by use of a uniform-phase LO obtained by splitting out the input pump beam and by applying a linear phase shift on the LO. In contrast, a Gaussian pump pulse has a position-dependent intensity profile I_p under the pulse's spatial–temporal envelope, resulting in position-dependent values for $-2\kappa_p I_p l$ and $\Phi_{ab}(I_p)$. In this case, if a uniform-phase LO pulse is used the SSD phase can be matched at certain points, say, at the peak point of the pulse, whereas at all the other points the SSD phase is mismatched. As a result the LO will pick up the squeezed quadrature at its pulse center and some degree of the antisqueezed quadrature (i.e., noise) off the LO pulse center. This additional noise will reduce the amount of squeezing substantially.

The effect of pump–probe phase mismatch $\Delta\kappa$ on squeezing is embedded in variables a, b, and c in Eq. (18). From Eqs. (19)–(22) and (A1)–(A6) below one can see that these variables are complicated functions of $\Delta\kappa$, and thus the effect of $\Delta\kappa$ is not obvious from the equations. It is studied numerically in Subsection 4.A.1.

4. DISCUSSION AND NUMERICAL RESULTS

From the above discussion we know that there are three factors that potentially limit the amount of squeezing achievable: pump–probe phase mismatch, SSD phase mismatch, and nonlinear absorption. The effects of pump–probe phase mismatch and nonlinear absorption exist for any type of pump pulse, including cw pump. The effect of SSD phase mismatch is present for either Gaussian pulses or any other pulses without uniform intensity profiles when a uniform-phase LO pulse is used. In this section we discuss these three effects through numerical analysis. In the analysis we use the parameters measured in Ref. 27. These are, for the $\mathrm{Al}_x\mathrm{Ga}_{1-x}\mathrm{As}$ waveguide at wavelength $\lambda = 1.55$ μm, two-photon absorption coefficient $\alpha^{(2)} = 0.26 \times 10^{-4}$ cm/MW, three-photon absorption coefficient $\alpha^{(3)} = 0.004$ cm^3/GW^2, and nonlinear refractive index $n^{(2)} = (3.6 \pm 0.5) \times 10^{-14}$ cm^2/W. When the pump and the probe beams have the same polarization, $\kappa_s = (4\pi/\lambda)n^{(2)}$ and $\gamma = 2[\alpha^{(2)} + \alpha^{(3)}I_p]I_p$. To simplify the discussion we first present the case in which the nonlinear absorption is neglected and then discuss the effect of nonlinear absorption. For the purpose of discussion we choose a typical pump pulse peak intensity of 4.5 GW/cm^2, which can be achieved in a laboratory.

A. Case 1: Without Nonlinear Absorption

1. Pump–Probe Phase Mismatch
To see the effect of pump–probe phase mismatch only, we choose a square pulse as the pump pulse because it does not have SSD phase mismatch. In this case we calculate the amount of squeezing by using Eqs. (18) and (23) and take the LO pulse to be a uniform-phase square pulse with the same pulse width as that of the pump.[31] To find the quadrature that gives maximum amount of squeezing,
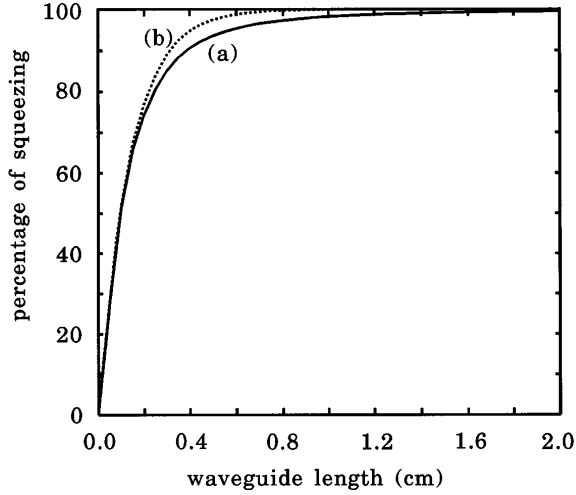
Fig. 2. Effect of nonlinear pump–probe phase mismatch $\Delta\kappa$ on the amount of squeezing as function of waveguide length for a square pump pulse with 4.5-GW/cm^2 pulse peak intensity, uniform-phase LO pulse, and no nonlinear absorption: (a) $\Delta\kappa \neq 0$ calculated with $\Delta\kappa = 2(\kappa_s - \kappa_p)I_p$ and the parameters given in the text; (b) $\Delta\kappa = 0$.

that is, the value of φ in Eq. (23) that maximizes S, we vary φ numerically until we obtain the maximum value for S. Figure 2 shows the results of our numerical calculations using a square pump pulse with a pulse peak intensity of 4.5 GW/cm^2. For curve (a) the pump–probe phase mismatch was taken into account [$\Delta\kappa \neq 0$, with $\Delta\kappa = 2(\kappa_s - \kappa_p)I_p$ and its value calculated with the parameters given in the text]; for curve (b) we removed it by setting $\Delta\kappa = 0$. Comparing these two curves, one can see that in the short-waveguide region the amount of squeezing is reduced by less than 5% by pump–probe phase mismatch, whereas for long-waveguide length the maximum amount of squeezing approaches 100% in both cases with no apparent difference between them. Hence the pump–probe phase mismatch reduces the effective interaction strength but does not limit the amount of squeezing achievable. We now discuss the amount of squeezing achievable with a Gaussian pump pulse, which describes more closely the pulses obtained experimentally in the laboratory.

2. Squeezed-State Detection Phase Mismatch
As discussed above, a Gaussian pump pulse with a uniform-phase LO pulse will result in SSD phase mismatch. The intensity profile of the Gaussian pump pulse is described by

$$I_p(z_c) = I_p(0)\exp(-z_c{}^2),   (25)$$

where $I_p(0)$ is the pulse peak intensity and we have normalized the Gaussian pulse width to be 1, with z_c the normalized distance to the pulse center. In all the numerical calculations for Gaussian pulses in this paper, $I_p(0)$ is taken to be 4.5 GW/cm^2. To take into account the effect of SSD phase mismatch, we carried out our numerical analysis by dividing the Gaussian pulse into many slices parameterized by z_c. Each slice is approximated by a square pulse. The contribution to photocurrent fluctuations from each slice is calculated as described above with Eqs. (18) and (23). Let the contribution from

the slice at z_c be $S(z_c)$; then the net squeezing for the whole pulse S_{tot} is given as follows:

$$S_{\text{tot}} = \frac{\sum_j S(z_{cj})I_{\text{LO}}(z_{cj})}{\sum_j I_{\text{LO}}(z_{cj})},   (26)$$

where $\sum_j$ denotes the sum over each slice. Note that, as the pulse propagates down the waveguide, each slice sees a different pump phase because of the pump's self-phase modulation. The pump's self-phase modulation is given by $\kappa_p I_p(z_c)l$, which is dependent on the location z_c of the slice inside the pulse. For the case when the LO phase φ is uniform (i.e., $\varphi = $ constant), different slices of the Gaussian pulse will experience different amounts of SSD phase mismatch, resulting in a deterioration in the amount of squeezing detected. We first consider the case in which the LO pulse is also chosen to be a Gaussian pulse with the same width as the pump but with uniform phase φ. We obtained the maximum amount of squeezing achievable as a function of waveguide length by varying the LO phase as before. Figure 3 shows that in this case the maximum amount of squeezing achievable is ~50%, as illustrated by curve (a), and, as the waveguide length increases, the effect of SSD phase mismatch is so strong that the amount of squeezing goes to zero. As discussed above, this drastic decrease in squeezing is attributed to noise that comes from the antisqueezed quadrature because of SSD phase mismatch.

By choosing either a narrow or a matched LO pulse we expect to improve the amount of squeezing achievable. We now repeat our calculations, using a narrow LO pulse with a width narrower than that of a squeezed vacuum pulse, and overlap the center of the LO pulse with that of the squeezed vacuum pulse. In this case the SSD phase-matching condition can be satisfied in the neighborhood of the pulse center. Squeezing will be detected in this region, and noise will be ignored at all other places. Physically this means that the narrow LO pulse sees the overlapping region as approximately a square pulse. Curves (b), (c), and (d) of Fig. 3 show the results for a
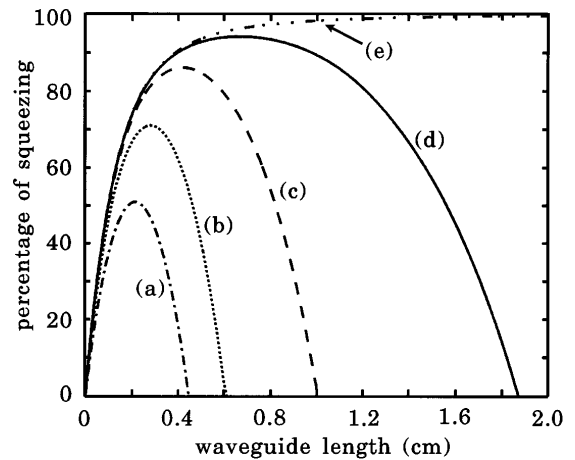
Fig. 3. Effect of SSD phase mismatch on squeezing for a Gaussian pump pulse with uniform phase under its pulse profile and without nonlinear absorption: (a) the LO pulse has the same width as the Gaussian pump pulse; (b), (c), (d) narrow uniform-phase LO pulses, where the LO pulse width is taken to be one half, one fourth, and one eighth, respectively, of that of the pump pulse. (e) The square pump pulse case for comparison.

uniform-phase Gaussian LO pulse with pulse widths one half, one fourth, and one eighth, respectively, of that of the Gaussian pump pulse. In the case illustrated by curve (d) we see that for short-waveguide length the maximum amount of squeezing is close to 95%, approaching the ideal square pump pulse case, which is illustrated in curve (a) of Fig. 2 and reproduced in curve (e) of Fig. 3. For long-propagation-medium length the amount of squeezing decreases, departing from the asymptote observed for the square pulse case, possibly because the LO pulse begins to pick up the antisqueezed components as the pump undergoes further self-phase modulation.

Another way to overcome SSD phase mismatch is to choose a matched LO pulse[25,32] that provides matched nonlinear phase variation such that the SSD phase-matching condition described by Eq. (24) is satisfied for the entire pulse. From the above discussion one can see that the phase variation that needs to be matched is the sum of $-2\kappa_p I_p l$ and Φ_{ab}. By studying the characteristics of these two nonlinear phase variations we can find the requirement for a matched LO pulse.

As was pointed out above, the term $-2\kappa_p I_p l$ originates from the nonlinear phase shift of the pump, so it has Gaussian variation across the whole pulse. The $\Phi_{ab}(I_p)$ term, on the other hand, given by $\Phi_{ab}(I_p) = \arctan(a/b) = \arctan[\mathrm{Re}(\mu\nu)/\mathrm{Im}(\mu\nu)] = -\mathrm{Arg}(\mu\nu)$, originates from pump intensity dependence of the four-wave mixing process but has an indirect dependence on the pump intensity I_p through the parameters a and b. (Remember that losses and Langevin noises are not considered here.) Figure 4 shows the variation of $\Phi_{ab}(I_p)$ across the whole Gaussian pump pulse as a function of waveguide length. We see that for short-waveguide length the variation of $\Phi_{ab}(I_p)$ across the whole pulse is similar to that of the Gaussian pump pulse intensity profile. However, as the waveguide length increases, $\Phi_{ab}(I_p)$ becomes saturated around the peak intensity. Figure 5 shows the relative values of $\Phi_{ab}(I_p)$ [curve (a)], $-2\kappa_p I_p l$ [curve (b)], and their sum [curve (c)] at the pump pulse center as a function of the waveguide length l. From the curves we can see that the magnitude of the term $-2\kappa_p I_p l$ is several times larger than that of the $\Phi_{ab}(I_p)$ term at the same pump intensity I_p, and hence the effect of the former is dominant [e.g., at $l > 0.4$ cm, $2\kappa_p I_p l > 3\Phi_{ab}(I_p)$]. From Figs. 4 and 5 one can see that it is not trivial to produce a LO pulse whose phase variation exactly matches both $-2\kappa_p I_p l$ and $\Phi_{ab}(I_p)$ or their sum because of the non-Gaussian variation of Φ_{ab}. However, it is possible to obtain two kinds of LO pulse that can give fairly good results:

(i) Output pump pulse from the same waveguide (reused pump pulse): In this case the nonlinear phase variation of this LO pulse matches exactly the phase variation that is due to the $-2\kappa_p I_p l$ term and can therefore reduce the effect of SSD phase mismatch considerably. Specifically, the phase of the LO pulse in this case is also dependent on pulse position z_c and can be written as

$$\varphi(z_c) = \varphi_c + \kappa_p I_p(z_c) l, \qquad (27)$$

where φ_c is the constant part and $\kappa_p I_p(z_c) l$ is provided by the waveguide. Substitute Eq. (27) into Eq. (24); it can be seen that the nonlinear phase shift of the pump is can-

celed out. In the numerical calculation we vary the value of φ_c to minimize S_tot given by Eq. (26). (This physically simulates the translation of the piezoelectric mirror used to shift the LO phase.) The results are shown in curve (a) of Fig. 6, for which we assume that the LO pulse has the same pulse width as that of the pump pulse. It is shown that ~86% squeezing can be achieved in this case. This maximum amount of squeezing is still lower than what was obtained for the square pump pulse case, and it reflects the fact that corrections to the SSD phase mismatch were not complete.

(ii) Output pump pulse from a second waveguide: In this case we use a waveguide with the same characteristics as the one used for the generation of squeezing, except that it has a different length. We find that besides the $\kappa_p I_p l$ term this new waveguide can provide an additional nonlinear phase shift for the LO pulse, thus minimizing the effect of Φ_{ab}. Experimentally we accomplish this by splitting the pump pulse into two beams, using a 50:50 beam splitter. One beam is sent into the waveguide for the generation of squeezing, and the other is sent into the second waveguide to produce the LO pulse. For clarity, let us keep the same notation by calling the first beam the pump pulse and the second beam the LO pulse. We correspondingly call the first waveguide the squeezing wave-
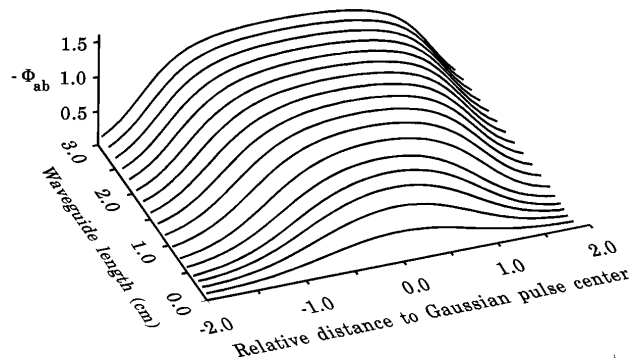
Fig. 4. Variation of $-\Phi_{ab}$ across the Gaussian pump pulse as a function of waveguide length.
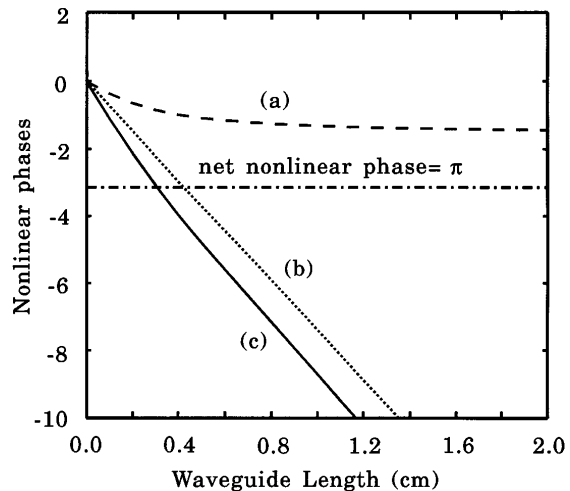
Fig. 5. Waveguide length dependence of the nonlinear phase terms Φ_{ab} (dashed curve) and $-2\kappa_p I_p l$ (dotted curve) at the pump pulse center. The solid curve represents their difference $-2\kappa_p I_p l + \Phi_{ab}$. The dotted–dashed line corresponds to phase π.
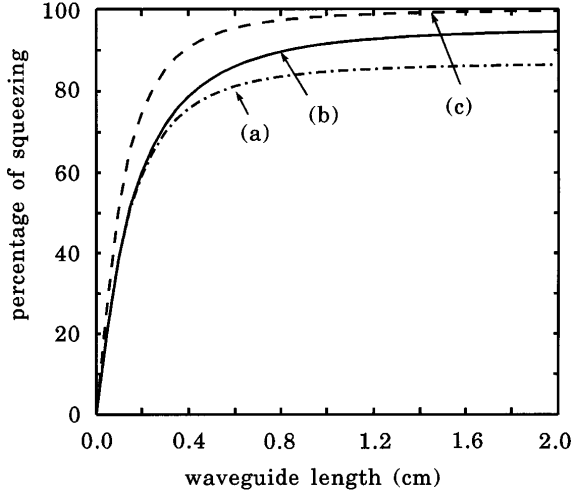
Fig. 6. Improved detection of squeezing with two kinds of matched LO pulse: (a) output pump pulse from the same waveguide, (b) optimal LO pulse from another waveguide. (c) For comparison, we also show the square pump pulse.

guide and the second one the LO waveguide. The LO waveguide length is l', and it is related to the squeezing waveguide length l by $l' = l + \Delta l$. In this case the phase shift of the LO pulse can be written as

$$\varphi(z_c) = \varphi_c + \kappa_p I_p(z_c) l'$$
$$= \varphi_c + \kappa_p I_p(z_c) l + \kappa_p I_p(z_c) \Delta l, \qquad (28)$$

where the second term $\kappa_p I_p(z_c) l$ on the right-hand side matches exactly the pump nonlinear phase shift and the third term $\kappa_p I_p(z_c) \Delta l$ can be used to minimize the effect of Φ_{ab} by optimizing Δl. We shall call such a LO pulse a nearly matched LO pulse and this scheme a two-waveguide squeezer. In this case 95% squeezing can be achieved, as illustrated by curve (b) of Fig. 6. Note that when the reused pump LO pulse or the nearly matched LO pulse is used, as described by curves (a) and (b) of Fig. 6, the amount of squeezing as a function of waveguide length follows the general behavior of curve (c), which describes the case of a square pump pulse and is the reproduction of curve (a) of Fig. 2. These results are in contrast to those obtained with uniform-phase Gaussian LO pulses [see curves (a) and (b) of Fig. 3].

Actually, if the two waveguides have exactly the same length, the LO pulse can be optimized in another way, i.e., by optimizing the intensity of the LO pulse. The principles are the same, except that the extra nonlinear phase variation is provided by the intensity difference between the LO pulse and the pump pulse.

B. Case 2: Effect of Nonlinear Absorption
One can see more clearly the effect of nonlinear absorption on the amount of squeezing achievable by analyzing two limiting cases: $\gamma l \ll 1$ (i.e., when the product of nonlinear absorption and waveguide length is much smaller than unity) and $\gamma l \gg 1$. The results are investigated numerically. To understand the results, we also derive the results analytically in Appendix A with appropriate approximations. These results are discussed in the following subsections.

1. Small Nonlinear Absorption $\gamma l \ll 1$
Small nonlinear absorption corresponds to a $\chi^{(3)}$ medium with a small nonlinear absorption coefficient or to a relatively short $\chi^{(3)}$ medium. Figure 7 shows the results for a square pulse and Gaussian pulses with various LO pulses when the pump and the probe beams have parallel polarizations. These numerical results are obtained in the same way as for Fig. 6, except that nonlinear absorption is taken into consideration here. Curves (a)–(d) are results of a Gaussian pump pulse with different LO pulses. Curve (a) is for the nearly matched LO pulse. In curve (b) the LO pulse is a reused pump pulse. In curve (c) the LO pulse is a uniform-phase Gaussian pulse with a width narrower than that of the pump pulse (one eighth of the pump pulse width). In curve (d) the LO pulse is simply a Gaussian pulse with uniform phase and the same width as the pump pulse. Curve (e) is the result of a square pump pulse. To see the nonlinear loss at different waveguide lengths simultaneously, we included the percentage of probe absorption as curve (f). By comparing Figs. 6 and 7 one can see the following: (i) For all curves, when the nonlinear phase shift is small (i.e., $X_r l \ll 1$ in the small-waveguide length region $l < 0.1$ cm), the effect of nonlinear absorption can be neglected, and the amount of squeezing increases linearly with the nonlinear phase shift. This is manifested by the analysis in Appendix A [see Eq. (A20)]. (ii) As the waveguide length increases, the effect of nonlinear absorption becomes important. From Eq. (A24) one can see that, when the nonlinear phase shift is large (i.e., $X_r l \gg 1$) but nonlinear absorption is still small, the nonlinear absorption reduces squeezing by the percent of nonlinear probe absorption. This is verified in curves (a)–(d) of Fig. 7 at 0.1 cm $< l <$ 0.5 cm, where the nonlinear absorption is less than 10%. For waveguide length $l > 0.5$ cm the nonlinear absorption becomes so large that the relation between the amount of squeezing and the nonlinear absorption is not linear, and the squeezing behavior cannot be simply predicted by Eq. (A24) in this case. For curves (a)–(c), where there is no SSD
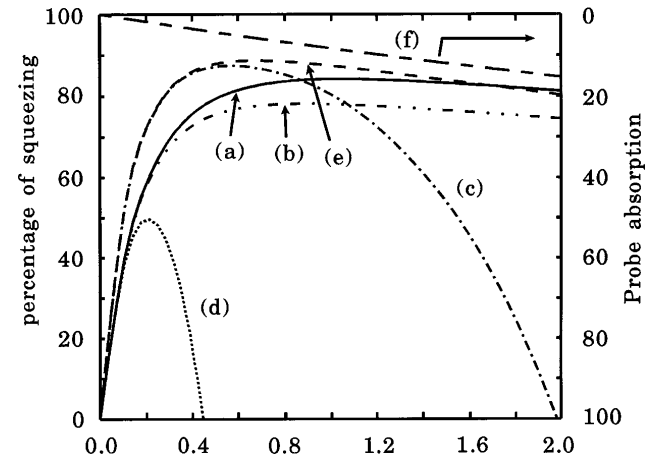
Fig. 7. Squeezing with nonlinear absorption: (a) Gaussian pump pulse with a nearly matched LO pulse from another waveguide, (b) Gaussian pump pulse with a reused pump pulse, (c) Gaussian pump pulse with a narrower uniform-phase LO pulse, (d) Gaussian pump pulse with a uniform-phase LO pulse having the same pulse width as the pump, (e) square pump pulse. (f) Relative pump amplitude $E_p(l)/E_p(0)$.

phase mismatch or the SSD phase mismatch is minimum, the squeezing curves still approximately follow the nonlinear absorption curve (f). One interesting phenomenon to be noted here is that, at long-waveguide length ($l > 1.8$ cm), the squeezing observed for the case of a Gaussian pump pulse with a nearly matched LO pulse [curve (a)] is slightly larger than that for the square pump pulse [curve (e)]. The reason for this small improvement is probably that a square pulse has the same high intensity for the whole pulse and therefore the total nonlinear absorption experienced by the whole probe pulse is larger than that experienced for the case of a Gaussian pump pulse. For curve (d) of Fig. 7, where a narrower LO pulse is used, the squeezing curve initially follows the loss curve somewhat but deteriorates rapidly as the waveguide length increases. Also, for curve (e), where the pump is a Gaussian pulse and LO is a uniform-phase Gaussian pulse, the effect of the nonlinear absorption is not obvious, as the amount of squeezing deteriorates to zero before the amount of absorption becomes substantial.

From Fig. 7 we find that, even with nonlinear absorption, for the case of a Gaussian pump pulse ~85% squeezing can be achieved when a narrow or nearly matched LO pulse is used.

2. Large Nonlinear Absorption $\gamma l \gg 1$

Next we describe the limit of a $\chi^{(3)}$ medium with large nonlinear absorption. From Eq. (A34) in Appendix A one can see that in the limit of a long medium the amount of squeezing achievable is a constant S_∞, whose value depends only on the ratio of the nonlinear coupling coefficient to the nonlinear absorption, i.e., $R = (X_r I_p/\gamma)$. Actually R is determined by the ratio $n^{(2)}/\alpha^{(2)}$. When three-photon absorption is negligible, R is related to the factor of merit F by $R = 1/(2\pi F)$ [See Eq. (A38)]. Figure 8 shows the numerical results of Eq. (A34), and one can see that in the limit of very large nonlinear absorption, i.e., $R \to 0$, more than 33% of squeezing can still be achieved without SSD phase mismatch, whereas for smaller nonlinear absorption satisfying the condition $\gamma l \gg 1$ (resulting in large R, e.g., $R > 14.0$) the final amount of squeezing achieved will be 50%. The nonzero amount of squeezing in the long-medium limit is due to the fact that nonlinear absorption as well as nonlinear coupling coefficient X_s contributes to pure loss because of the formation of the nonlinear loss grating. In Fig. 9 we calculate the amount of squeezing achievable by a Gaussian pump pulse with a matched LO pulse for a waveguide length up to 50 cm for three different ratios R. The solid and the dashed curves have $R = 16.5$ and $R = 33$, respectively. As expected, the amount of squeezing achievable in a long waveguide is a constant of 50%. The dotted curve corresponds to the case with $R = 0.01$, and the limit of squeezing is ~33%, which is consistent with Fig. 8.

In the above discussion we neglected the reduction of pump intensity that results from nonlinear absorption as it propagates through the medium and assumed that the intensity is constant in the whole medium. Actually, $I_p(l) = I_p(0)\exp(-\gamma l)$, and the assumption is valid for the case when $\gamma l \ll 1$ (in our numerical calculation the reduction of pump intensity is less than 15% in this case), but

it is invalid for the case when $\gamma l \gg 1$ because then the pump is totally absorbed by the medium. However, the case when $\gamma l \gg 1$ is still important because it gives insight into the effect of nonlinear absorption on squeezing. It represents the steady-state situation in which squeezing occurs at the output end of the waveguide within a length roughly given by the absorption length of the medium.

5. CONCLUSIONS

In this paper we have examined in detail the feasibility of using a short $Al_xGa_{1-x}As$ semiconductor waveguide with $\chi^{(3)}$ nonlinearity to generate squeezing. An $Al_xGa_{1-x}As$ waveguide has the advantage over fiber in that GAWBS noise is negligible. To avoid two-photon absorption, which can be large close to the band-gap energy of $Al_xGa_{1-x}As$, we considered the wavelength regime below the half-band-gap energy. We found that
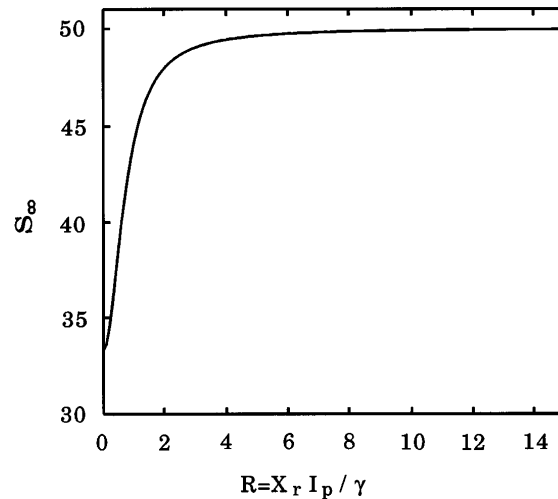
Fig. 8. Limit of the amount of squeezing S_∞ for different ratios $R = X_r I_p/\gamma$ when $\gamma l \gg 1$.
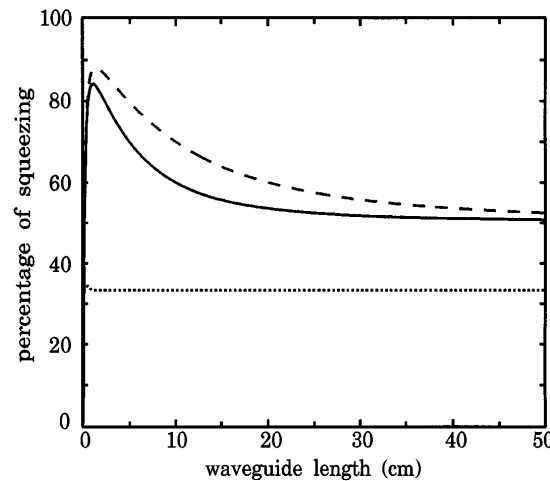
Fig. 9. Amount of squeezing achievable in a long waveguide for different ratios R. The pump pulse is a Gaussian pulse, and the LO pulse is a matched one optimized in another waveguide. Solid curve, $R = 16.5$; dashed curve, $R = 33$; dotted curve, $R = 0.01$. All other parameters are the same as those that we use for the practical waveguide discussed through this paper and in Ref. 27.

in that regime a reasonably large amount of squeezing can be achieved. Our theoretical analysis took into account various effects that can affect squeezing. They include (i) nonlinear pump–probe phase mismatch, (ii) nonlinear absorption, and (iii) squeezed-state detection (SSD) phase mismatch. The first two factors affect the amount of squeezing generated, whereas the third factor affects the amount of squeezing detected. We found that the effect of nonlinear pump–probe phase mismatch does not impose a fundamental limit on the amount of squeezing achievable and can be easily overcome by use of a long medium length or a higher pump intensity. The effect of nonlinear absorption, however, reduces the maximum amount of squeezing achievable by an amount that is roughly equal to the percent of absorption. The SSD phase mismatch exists only for pulsed squeezed-state light generated by a nonsquare pump pulse, and it can seriously affect the maximum amount of squeezing detected. We pointed out that the SSD phase mismatch has two contributions, one from the pump's self-phase modulation and the other from the nature of the four-wave mixing interaction. We showed that if the pump pulse is a Gaussian pulse and if the LO pulse is an ordinary unchirped pulse that has a uniform phase under its pulse profile (called a uniform-phase LO), then because of SSD phase mismatch only 50% squeezing can be observed (compared with >99% squeezing in the case when the pump is a square pulse for which there is no SSD phase mismatch). This is so even for the ideal case in which the medium has no loss. We then discussed three methods to overcome the effect of SSD phase mismatch, namely, (i) the use of a narrow LO pulse (narrow LO scheme), (ii) the use of the pump pulse after the medium as the LO pulse (reused pump scheme), and (iii) the use of a separate nonlinear waveguide to generate a LO pulse (separate waveguide LO scheme). We analyzed the maximum amount of squeezing detectable for these three types of LO (assuming a Gaussian pump pulse) for the case in which absorption is neglected. We showed that obtaining a substantial advantage with the narrow LO scheme requires that the LO pulse width be $\lesssim 1/8$ that of the pump pulse, for which as much as 95% squeezing can be observed (compared with 50% for the case of a uniform-phase LO); with the reused pump pulse as the LO pulse (reused pump LO scheme) as much as 85% of squeezing can be observed; and with the use of a separate nonlinear waveguide to optimize the phase matching between the phase profile of the LO pulse and the squeezed-state light pulse (separate waveguide LO scheme) as much as 95% of squeezing can be observed. We call the LO pulse generated with the separate waveguide LO scheme the nearly matched LO pulse, as it allows us to cancel out completely the part of SSD phase mismatch that is due to pump's self-phase modulation and partially to cancel out the part of SSD phase mismatch that is due to the nature of the four-wave mixing interaction. We pointed out that the LO pulse generated with the reused pump LO scheme enables one to cancel out only the part of the SSD phase mismatch that is due to the pump's self-phase modulation and hence is not so good as the nearly matched LO pulse. The reused pump LO scheme was used recently to optimize the amount of squeezing detected in the case of a fiber squeezer.

Finally we included the two-photon absorption and three-photon absorption effects in the $Al_xGa_{1-x}As$ semiconductor waveguide. We found that the effect of nonlinear absorption is dominated by two-photon absorption and in the worst case gives a 10% reduction in the maximum amount of squeezing observable. When nonlinear absorption effects are included, one of the best schemes to achieve large amounts of squeezing is the separate waveguide LO scheme. In that case the maximum amount of squeezing achievable with a 1-cm-long waveguide and a pump pulse peak intensity of 4.5 GW/cm^2 is ~85% (compared with 79% with the reused pump pulse LO scheme). The narrow LO pulse scheme can give a similar amount of squeezing but may be harder to realize in practice if the pump pulse is already very narrow, because then it will be difficult to generate an even narrower pulse.

APPENDIX A. EFFECT OF NONLINEAR ABSORPTION

To see the effect of nonlinear absorption clearly we simplify Eq. (18) in two cases: $\gamma l \ll 1$ and $\gamma l \gg 1$.

Case 1: $\gamma l \ll 1$

First let us write the expressions for Re($\mu\nu$), Im($\mu\nu$), Re($\Gamma_1\Gamma_2$), Im($\Gamma_1\Gamma_2$), $|\nu|^2$, and $\langle\Gamma_1^\dagger\Gamma_1\rangle$ in Eqs. (19)–(22):

$$\text{Re}(\mu\nu) = -\frac{X_i I_p}{2\Omega}\sinh(2\Omega l) - \frac{X_r I_p \Delta\kappa}{2\Omega^2}\sinh^2(\Omega l),$$
(A1)

$$\text{Im}(\mu\nu) = -\frac{X_r I_p}{2\Omega}\sinh(2\Omega l) - \frac{\Delta\kappa X_i I_p}{2\Omega^2}\sinh^2(\Omega l),$$
(A2)

$$\begin{aligned}\text{Re}(\Gamma_1\Gamma_2) = &-2\gamma(2\bar{n}+1)\Bigg(\frac{X_i I_p}{8\Omega}\Bigg\{\frac{\exp[2(\Omega-\gamma)l]-1}{\Omega-\gamma}\\ &+\frac{\exp[-2(\Omega-\gamma)l]-1}{\Omega+\gamma}\Bigg\}+\frac{X_r I_p\Delta\kappa}{8\Omega^2}\\ &\times\Bigg\{\frac{\exp[2(\Omega-\gamma)l]-1}{\Omega-\gamma}\\ &-\frac{\exp[2(\Omega-\gamma)l]-1}{\Omega+\gamma}+\frac{\exp(-2\gamma l)-1}{\gamma}\Bigg\}\Bigg),\end{aligned}$$
(A3)

$$\begin{aligned}\text{Im}(\Gamma_1\Gamma_2) = &\ 2\gamma(2\bar{n}+1)\Bigg(\frac{X_r I_p}{8\Omega}\Bigg\{\frac{\exp[2(\Omega-\gamma)l]-1}{\Omega-\gamma}\\ &+\frac{\exp[-2(\Omega-\gamma)l]-1}{\Omega+\gamma}\Bigg\}-\frac{X_i I_p\Delta\kappa}{8\Omega^2}\\ &\times\Bigg\{\frac{\exp[2(\Omega-\gamma)l]-1}{\Omega-\gamma}\\ &-\frac{\exp[-2(\Omega-\gamma)l]-1}{\Omega+\gamma}\\ &+\frac{2[\exp(-2\gamma l)-1]}{\gamma}\Bigg\}\Bigg),\end{aligned}$$
(A4)

$$|\nu|^2 = \frac{|X_s I_p|^2}{\Omega^2}\sinh^2(\Omega z),$$
(A5)

$$\langle \Gamma_1^\dagger \Gamma_1 \rangle = \frac{1}{4}\, \gamma \bar{n} \Biggl[\frac{\exp[2(\Omega - \gamma)l] - 1}{\Omega - \gamma}$$

$$- \frac{\exp[-2(\Omega - \gamma)l] - 1}{\Omega + \gamma}$$

$$- \frac{2[\exp(-2\gamma l) - 1]}{\gamma} \Biggr] \Biggr)$$

$$+ \Biggl[2\gamma \bar{n} \left(\frac{\Delta \kappa}{2\Omega} \right)^2 + 2\gamma (\bar{n} + 1) \left(\frac{|X_s I_p|}{\Omega} \right)^2 \Biggr]$$

$$\times \Biggl\{ \frac{\exp[2(\Omega - \gamma)l] - 1}{\Omega - \gamma}$$

$$- \frac{\exp[-2(\Omega - \gamma)l] - 1}{\Omega + \gamma}$$

$$+ \frac{2[\exp(-2\gamma l) - 1]}{\gamma} \Biggr\}, \tag{A6}$$

where X_r and X_i are the real part and the imaginary part, respectively, of nonlinear coupling coefficient X_s, $\bar{n}$ is the average thermal photon number, and, from Eqs. (1)–(3),

$$X_r = \kappa_p = \frac{2\pi}{\lambda}\, n^{(2)}, \qquad X_i = \frac{\gamma}{2I_p}. \tag{A7}$$

On the other hand, for parallel polarization

$$\Delta \kappa = 2(\kappa_s - \kappa_p) I_p = 2 X_r I_p. \tag{A8}$$

So one can obtain $\Omega = \gamma/2$.

Assume that $\gamma l \ll 1$ (the absolute nonlinear absorption is small); then to the first order of γl one can obtain

$$\text{Re}(\mu \nu) \simeq -(X_r I_p l)^2 - \tfrac{1}{2}(\gamma l), \tag{A9}$$

$$\text{Im}(\mu \nu) \simeq (X_r I_p l) - \tfrac{1}{2}(X_r I_p l)(\gamma l), \tag{A10}$$

$$\text{Re}\langle \Gamma_1 \Gamma_2 \rangle \simeq -\tfrac{2}{3}(X_r I_p l)^2 (\gamma l), \tag{A11}$$

$$\text{Im}\langle \Gamma_1 \Gamma_2 \rangle \simeq (X_r I_p l)(\gamma l), \tag{A12}$$

$$\langle \Gamma_1^\dagger \Gamma_1 \rangle \simeq \tfrac{2}{3}(X_r I_p l)^2 (\gamma l), \tag{A13}$$

$$|\nu|^2 = (X_r I_p l)^2. \tag{A14}$$

Then

$$a \simeq -(X_r I_p l)^2 + [\tfrac{4}{3}(X_r I_p l)^2 - \tfrac{1}{2}](\gamma l), \tag{A15}$$

$$b \simeq (X_r I_p l) - \tfrac{3}{2}(X_r I_p l)(\gamma l), \tag{A16}$$

$$c \simeq (X_r I_p l)^2 [1 - \tfrac{4}{3}(\gamma l)]. \tag{A17}$$

Here we discuss two cases: (i). Small nonlinear phase shift, i.e., $(X_r I_p l) = \kappa_p I_p l \ll 1$. Then

$$\sqrt{a^2 + b^2} = (X_r I_p l)\{1 + [(-\tfrac{1}{2}\gamma l)$$

$$+ (X_r I_p l)^2 (1 - \tfrac{8}{3}\gamma l)]\}^{1/2}$$

$$\simeq (X_r I_p l) - \tfrac{1}{4}(X_r I_p l)(\gamma l). \tag{A18}$$

Suppose that the phase is perfectly matched for homodyne detection (this is correct in the case of a square pump pulse or Gaussian pump pulse with matched LO), i.e.,

$\sin(2\varphi - 2\kappa_p I_p l + \alpha) = -1$; then the squeezed quadrature is

$$\langle [\Delta X(\varphi)]^2 \rangle = \tfrac{1}{4} + \tfrac{1}{2}(c - \sqrt{a^2 + b^2}),$$

$$\simeq \tfrac{1}{4} - \tfrac{1}{2}(X_r I_p l) \tag{A19}$$

and the amount of squeezing as a percent is

$$S = \{1 - 4\langle [\Delta X(\varphi)]^2 \rangle\} \times 100\% = 2(X_r I_p l) \times 100\%,$$

$$= 2\kappa_p I_p l \times 100\%. \tag{A20}$$

One can see that, in this case, the amount of squeezing increases linearly with the increase of nonlinear phase shift of the pump or is simply the nonlinear phase shift of the probe pulse.

(ii). Large nonlinear phase shift, i.e., $(X_r I_p l) \gg 1$. Then

$$\sqrt{a^2 + b^2} = (X_r I_p l)^2 \{1 + [-\tfrac{8}{3}(\gamma l)$$

$$+ \frac{1}{(X_r I_p l)^2}(1 - \tfrac{1}{2}\gamma l)]\}^{1/2}$$

$$\simeq (X_r I_p l)^2 [1 - \tfrac{4}{3}(\gamma l)]. \tag{A21}$$

Also, if it is assumed that the phase is perfectly matched for homodyne detection, then

$$\langle [\Delta X(\varphi)]^2 \rangle \simeq \tfrac{1}{8}(\gamma l), \tag{A22}$$

and the amount of squeezing is

$$S = [1 - \tfrac{1}{2}(\gamma l)] \times 100\%. \tag{A23}$$

Because of nonlinear dispersion, the nonlinear absorption of the probe is also twice of that of the pump. Suppose that γ_p is the nonlinear absorption of pump; then $\gamma = 2\gamma_p$ and then

$$S = [1 - (\gamma_p l)] \times 100\%, \tag{A24}$$

which means that in this case the reduction of the amount of squeezing is simply the nonlinear absorption of the pump amplitude.

Case 2: $\gamma l \gg 1$

Here

$$\text{Re}\langle \Gamma_1 \Gamma_2 \rangle \simeq -\frac{1}{3} + \frac{2}{3} \left(\frac{X_r I_p}{\gamma} \right)^2, \tag{A25}$$

$$\text{Im}\langle \Gamma_1 \Gamma_2 \rangle \simeq \frac{X_r I_p}{3\gamma}, \tag{A26}$$

$$\exp(-2\gamma l)\text{Re}(\mu \nu) \simeq 0, \tag{A27}$$

$$\exp(-2\gamma l)\text{Im}(\mu \nu) \simeq 0, \tag{A28}$$

$$\exp(-2\gamma l)|\nu|^2 \simeq 0, \tag{A29}$$

$$\langle \Gamma_1^\dagger \Gamma_1 \rangle \simeq \tfrac{2}{3} \left(\frac{X_r I_p}{\gamma} \right)^2 + \frac{1}{6}, \tag{A30}$$

and, if we let $R = X_r I_p/\gamma$, then

$$a = \exp(-2\gamma l)\text{Re}(\mu\nu) + \text{Re}\langle\Gamma_1\Gamma_2\rangle \simeq -\tfrac{1}{3} - \tfrac{2}{3}R^2, \quad \text{(A31)}$$

$$b = \exp(-2\gamma l)\text{Im}(\mu\nu) + \text{Im}\langle\Gamma_1\Gamma_2\rangle \simeq \tfrac{1}{3}R, \quad \text{(A32)}$$

$$c = \exp(-2\gamma l)|\nu|^2 + \langle\Gamma_1^\dagger\Gamma_1\rangle \simeq \tfrac{2}{3}R^2 + \tfrac{1}{6}. \quad \text{(A33)}$$

Assume perfect SSD phase matching; then

$$\langle[\Delta X(\varphi)]^2\rangle = \tfrac{1}{4} + \tfrac{1}{2}(c - \sqrt{a^2 + b^2})$$
$$= \tfrac{1}{4} + \tfrac{1}{2}\left\{(\tfrac{2}{3}R^2 + \tfrac{1}{6})\right.$$
$$\left. - \left[(-\tfrac{2}{3}R^2 - \tfrac{1}{3})^2 + \frac{R^2}{9}\right]^{1/2}\right\}. \quad \text{(A34)}$$

Here we also discuss two cases: (i). $R \ll 1$ or $\gamma \gg X_r I_p$. Then

$$\langle[\Delta X(\varphi)]^2\rangle = \tfrac{1}{4} + \tfrac{1}{2}\{(\tfrac{2}{3}R^2 + \tfrac{1}{6})$$
$$- \tfrac{1}{3}[1 + (4R^4 + 5R^2)]^{1/2}\}$$
$$\simeq \tfrac{1}{4} - \tfrac{1}{12}(1 + R^2), \quad \text{(A35)}$$

$$S = \tfrac{1}{3}(1 + R^2) \times 100\%. \quad \text{(A36)}$$

Note that, even when $R = 0$ ($X_r = 0$ or $\gamma \to \infty$), $S = 33\%$ can still be achieved.

(ii). $R \gg 1$ or $\gamma \ll X_r I_p$. Then

$$\langle[\Delta X(\varphi)]^2\rangle = \tfrac{1}{4} + \tfrac{1}{2}\left\{(\tfrac{2}{3}R^2 + \tfrac{1}{6}) - (\tfrac{1}{3} + \tfrac{2}{3}R^2)\right.$$
$$\left. \times \left[1 + \frac{R2/9}{(\tfrac{2}{3}R^2 +)^2\,\tfrac{1}{3}}\right]^{1/2}\right\}, \quad \text{(37)}$$

And then $S = 50\%$. The amount of squeezing achievable is always a constant.

Actually, if three-photon absorption is small, R is determined simply by the ratio of nonlinear refractive index to two-photon absorption coefficient, i.e., $n^{(2)}/\alpha^{(2)}$. From Eqs. (A7),

$$R = \frac{X_r I_p}{\gamma} = \frac{(2\pi/\lambda)n^{(2)}I_p}{2[\alpha^{(2)} + \alpha^{(3)}I_p]I_p} \simeq \frac{\pi}{\lambda}\frac{n^{(2)}}{\alpha^{(2)}}. \quad \text{(A38)}$$

Our discussion here shows that the limit of squeezing in a long $\chi^{(3)}$ medium is actually determined by the ratio $n^{(2)}/\alpha^{(2)}$. The larger the ratio, the larger the squeezing achievable in a long $\chi^{(3)}$ medium (limited to a maximum of 50%).

The above results are probably due to the fact that nonlinear absorption contributes to both pure loss and nonlinear coupling between the two noise sidebands because of the formation of the nonlinear loss grating.

ACKNOWLEDGMENT

REFERENCES AND NOTES

1. C. M. Caves, Phys. Rev. D **23,** 1693 (1981).
2. H. P. Yuen and J. H. Shapiro, IEEE Trans. Inform. Theory **IT-24,** 657 (1978).
3. R. E. Slusher and B. Yurke, J. Lightwave Technol. **8,** 466 (1990).
4. R. E. Slusher, L. W. Hollberg, B. Yurke, J. C. Mertz, and J. F. Valley, Phys. Rev. Lett. **55,** 2409 (1985).
5. R. M. Shelby, M. D. Levenson, S. H. Perlmutter, R. G. DeVoe, and D. F. Walls, Phys. Rev. Lett. **57,** 691 (1986).
6. Ling-An Wu, H. J. Kimble, J. L. Hall, and H. Wu, Phys. Rev. Lett. **57,** 2520 (1986).
7. M. W. Maeda, P. Kumar, and J. H. Shapiro, Opt. Lett. **3,** 161 (1986).
8. S. Machida, Y. Yamamoto, and Y. Itaya, Phys. Rev. Lett. **58,** 1000 (1987).
9. A. Heidmann, R. Horowicz, S. Reynaud, E. Giacobino, C. Fabre, and G. Camy, Phys. Rev. Lett. **59,** 2555 (1987).
10. S. T. Ho, N. C. Wong, and J. H. Shapiro, Opt. Lett. **16,** 840 (1991).
11. H. J. Kimble, Phys. Rep. **219,** 227 (1992).
12. S. T. Ho, P. Kumar, and J. H. Shapiro, J. Opt. Soc. Am. B **8,** 37 (1991).
13. M. D. Levenson, R. M. Shelby, and S. H. Perlmutter, Opt. Lett. **10,** 514 (1985).
14. G. P. Agrawal, *Nonlinear Fiber Optics* (Academic, New York, 1989), Chaps. 4 and 7.
15. R. M. Shelby, M. D. Levenson, and P. W. Bayer, Phys. Rev. B **31,** 5244 (1985).
16. K. Bergman, H. A. Haus, and M. Shirasaki, Appl. Phys. B **55,** 242 (1992).
17. R. M. Shelby, P. D. Drummond, and S. J. Carter, Phys. Rev. A **42,** 2966 (1990).
18. B. Yurke, P. Grangier, R. E. Slusher, and M. J. Potasek, Phys. Rev. A **35,** 3586 (1987).
19. R. E. Slusher, P. Grangier, A. LaPorta, B. Yurke, and M. J. Potasek, Phys. Rev. Lett. **59,** 2566 (1987).
20. K. Bergman, H. A. Haus, E. P. Ippen, and M. Shirasaki, Opt. Lett. **19,** 290 (1994).
21. K. Bergman and H. A. Haus, Opt. Lett. **16,** 663 (1991).
22. K. Bergman, H. A. Haus, E. P. Ippen, and M. Shirasaki, in *Annual Meeting,* Vol. 16 of 1993 OSA Technical Digest Series (Optical Society of America, Washington, D.C., 1993), pp. 142–143, paper WII1.
23. K. Bergman, C. R. Doerr, H. A. Haus, and M. Shirasaki, Opt. Lett. **18,** 643 (1993).
24. M. Shirasaki and H. A. Haus, Opt. Lett. **17,** 1225 (1992).
25. M. Shirasaki and H. A. Haus, J. Opt. Soc. Am. B **7,** 30 (1990). Also see Eq. (24) in this paper.
26. M. Rosenbluh and R. M. Shelby, Phys. Rev. Lett. **66,** 153 (1991).
27. S. T. Ho, C. E. Soccolich, M. N. Islam, W. S. Hobson, A. F. J. Levi, and R. E. Slusher, Appl. Phys. Lett. **59,** 2558 (1991).
28. Our initial experiments show that GAWBS noise is negligible in the semiconductor waveguide.
29. See Eq. (14), where $X_s = (1/2)[\kappa_s + i(\gamma/I_p)]$, and $\kappa_s = (4\pi/\lambda)n^{(2)}$.
30. In this case we can use the instantaneous model of the four-wave mixing process. See, e.g., L. G. Joneckis and J. H. Shapiro, J. Opt. Soc. Am. B **10,** 1102 (1993).
31. In the case of a square pump pulse, the shape of the LO pulse does not affect the amount of squeezing detectable as long as LO pulse has a uniform phase and its profile is enclosed in that of the square pump pulse.
32. O. Aytur and P. Kumar, Opt. Lett. **15,** 390 (1990).